JOC The Journal of Organic Chemistry

Article

pubs.acs.org/joc

Mesolysis of Radical Anions of Tetra-, Penta-, and Hexaphenylethanes

Sachiko Tojo, Mamoru Fujitsuka, and Tetsuro Majima*

The Institute of Scientific and Industrial Research (SANKEN), Osaka University, Mihogaoka 8-1, Ibaraki, Osaka 567-0047, Japan

Supporting Information

ABSTRACT: A central carbon−carbon (C−C) σ bond dissociation of polyphenylethane radical anions ($Ph_nE^{\bullet-}$, n = 3−6), mesolysis, was investigated by the transient absorption measurement during pulse radiolysis of Ph_nE in 2-methyltetrahydrofuran. The charge resonance (CR) band of 1,1,2,2-tetraphenylethane radical anion (1,1,2,2-$Ph_4E^{\bullet-}$) was observed in the near-infrared region immediately after an electron pulse to be attributed to the intramolecular dimer radical anion. The CR band disappeared with simultaneous formation of two absorption bands at 330 and 460 nm corresponding to diphenylmethyl radical and diphenylmethyl anion, respectively, indicating the occurrence of the mesolysis in 1,1,2,2-$Ph_4E^{\bullet-}$. During pulse radiolysis of 1,1,1,2,2,2-hexaphenylethane (Ph_6E), an absorption band of triphenylmethyl radical was observed at 340 nm immediately after an electron pulse. It is suggested that one electron attachment to Ph_6E is followed by the subsequent rapid C−C σ bond dissociation. Formation of intramolecular dimer radical anions in $Ph_nE^{\bullet-}$ such as 1,1,2-triphenylethane (Ph_3E), 1,1,1,2-tetraphenylethane (1,1,1,2-Ph_4E), and 1,1,1,2,2-pentaphenylethane (Ph_5E) was also studied together with the subsequent mesolysis. The mesolysis of $Ph_nE^{\bullet-}$ is discussed in terms of charge delocalization in the intramolecular dimer radical anions and the central C−C σ bond as well as bond dissociation energy of the central C−C σ bond of $Ph_nE^{\bullet-}$.

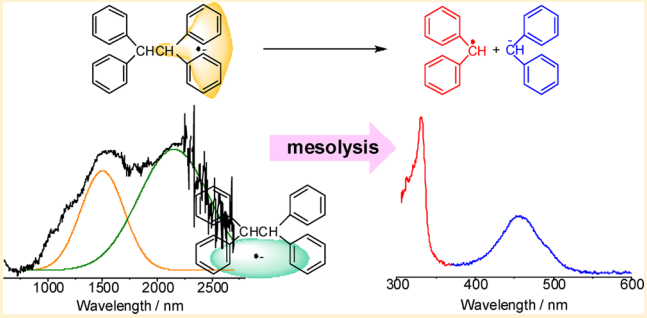

INTRODUCTION

Radical ions, generated from one electron oxidation or reduction of neutral molecules, are important reactive intermediates in organic, physical, inorganic, material, and biological chemistry. The dissociation of radical ions usually occurs more efficiently than the neutral molecules[1−5] to yield the corresponding radical and ion. The dissociation of various σ bonds such as carbon−carbon (C−C), carbon−sulfur (C−S), carbon−hydrogen (C−H), and carbon−silicone (C−Si) has been reported for radical cations of aromatic compounds ($M^{\bullet+}$) based on the transient absorption measurement during photolysis or radiolysis.[2,6−9] Compared with $M^{\bullet+}$, a small number of studies on the C−C σ bond dissociation has been reported for radical anions of aromatic compounds ($M^{\bullet-}$).[10] $M^{\bullet-}$ are usually generated either from chemical reductions using alkali metals or from electrochemical reactions. These classical methods are not suitable for the kinetic study on $M^{\bullet-}$, because $M^{\bullet-}$ are formed as contact pairs with metal ions, and not homogeneously. Pulse radiolysis is a powerful technique generating solvated electron (e_s^-) as a strong reducing agent, which selectively produces free radical anions of most substrate molecules.[11] Therefore, the kinetic information of free $M^{\bullet-}$ can be clearly obtained by pulse radiolysis.[12−14] Dissociative electron transfer (DET) is defined as one-electron reduction followed by σ-bond dissociation.[15−17] DET of 9-(phenoxymethyl)anthracene was found to occur via stepwise pathway involving the radical anion as an intermediate.[18] In the case of $M^{\bullet-}$ having polar carbon−heteroatom bonds such as polar carbon−halogen,[19,20] carbon−oxygen (C−O),[21−23] and C−S bonds,[24] the σ-bond dissociation of $M^{\bullet-}$ occurs efficiently to yield the corresponding carbon-centered radical and heteroatom anion. For example, the C−O σ bond dissociation of 4-nitrobenzyl phenyl ether radical anion (mesolysis) occurs with the mesolysis rate constant (k_{meso}) of 1.8×10^4 s^{-1}, while no mesolysis of nitrophenylphenylethane radical anion occurs at room temperature.[10,21,25] The mesolyses of C−S and S−S σ bonds have been observed for radical anions of nitrobenzyl phenyl sulfide[24] and dialkyl or diaryl disulfides,[26−28] respectively. In contrast, only a little is known on the C−C σ bond dissociation (mesolysis) of $M^{\bullet-}$.[10] When negative charge is delocalized in aromatic groups of $M^{\bullet-}$, $M^{\bullet-}$ can be more stable than radical anions of nonaromatic compounds. However, the mesolysis occurs often in such stabilized $M^{\bullet-}$. Maslak et al reported that one electron reduction of 1,1,2,2-tetraalkyl-1-(4′-nitorophenyl)-2-phenylethane is subsequently followed by the mesolysis.[1,10,29] The C−C σ bond dissociation is explained in terms of activation of the dissociation bond and charge delocalization including this bond in the transition state. However, the detailed mechanism of the C−C σ bond dissociation is still unclear. Recently, we showed that reduction

Special Issue: Howard Zimmerman Memorial Issue

Received: August 28, 2012
Published: November 27, 2012

of dinaphthyl disulfide having a nonpolar S−S bond provides a clear example of the mesolysis of dinaphthyl disulfide radical anion based on the transient absorption measurements during the pulse radiolysis.[28]

In the present study, we studied one electron reduction and the central C−C σ bond dissociation (mesolysis) of tri-, tetra-, penta-, and hexaphenylethanes (Figure 1) based on the transient absorption spectral measurement during the pulse radiolysis in 2-methyltetrahydrofuran (MTHF). The relationship between the structure and negative charge delocalization in such $Ph_nE^{\bullet-}$ is discussed.

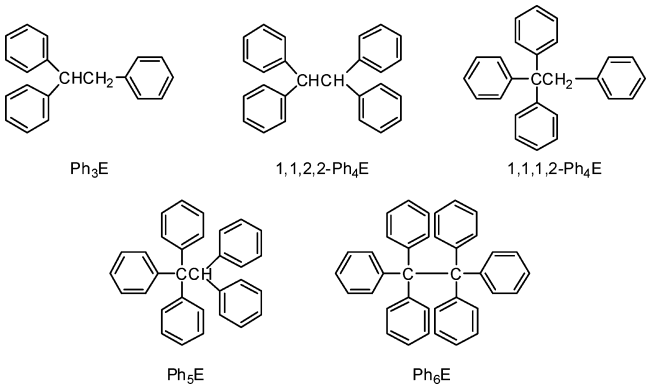

Figure 1. Tri, tetra-, penta-, and hexaphenylethanes studied in the present study. E, ethane.

RESULTS AND DISCUSSION

Mesolysis of 1,1,2,2-$Ph_4E^{\bullet-}$ and $Ph_3E^{\bullet-}$ Having 1,1-Diphenylmethyl Chromophore. One-electron reduction of polyphenylethanes (Ph_nE, n = 3−6) was carried out during the pulse radiolysis in degassed or Ar-saturated MTHF solution. The formation of $Ph_nE^{\bullet-}$ from the selective reduction of Ph_nE by e_s^- has been established in radiation chemical reaction (eqs 1−3).[11]

$$MTHF(C_5H_{10}O) \rightsquigarrow C_5H_{10}O^{\bullet+} + e_s^- \quad (1)$$

$$C_5H_{10}O + C_5H_{10}O^{\bullet+} \rightarrow C_5H_{10}OH^+ + {}^{\bullet}C_5H_9O \quad (2)$$

$$Ph_nE + e_s^- \rightarrow Ph_nE^{\bullet-} \quad (3)$$

The absorption spectrum of 1,1,2,2-$Ph_4E^{\bullet-}$ was measured after the γ-radiolysis of 1,1,2,2-Ph_4E in MTHF rigid glass at 77 K (Figure 2). No local excitation (LE) band was observed in the UV−visible region, while two intramolecular CR bands (A and B bands) were observed in the near-infrared (NIR) region to be assigned to 1,1- and 1,2-dimer radical anions between two phenyl groups of 1,1,2,2-$Ph_4E^{\bullet-}$ at 1,1- and 1,2-positions, respectively.[30] The negative charge of 1,1,2,2-$Ph_4E^{\bullet-}$ is delocalized on four phenyl groups at 77 K. The absorption spectral changes were observed for 1,1,2,2-$Ph_4E^{\bullet-}$ upon increasing temperature from 77 to 100 K. Increasing temperature to 80 K, 1,2-dimer radical anion (B band) at longer wavelength than 2200 nm disappeared, while 1,1-dimer radical anion (A band) at shorter wavelength than 2000 nm remained (Figure 2, dotted line). Further increasing temperature to 100 K, the A band also disappeared with no band formation.

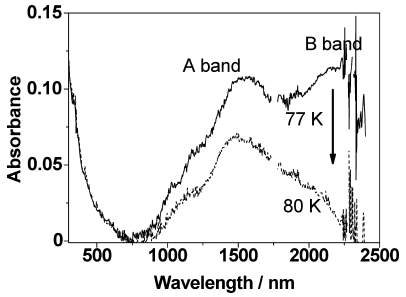

Figure 2. Absorption spectra observed after the γ-radiolysis of 1,1,2,2-Ph_4E (1.0×10^{-2} M) in MTHF rigid glass at 77 K and after increasing temperature to 80 K.

The transient absorption spectra were observed at various times after an 8-ns electron pulse during the pulse radiolysis of 1,1,2,2-Ph_4E in Ar-saturated MTHF at room temperature as shown in Figure 3. The A band of 1,1,2,2-$Ph_4E^{\bullet-}$ decayed in the time scale of 50 ns after a pulse with simultaneous formation of two absorption bands at 330 and 460 nm (Figure 3). The B band was not observed because the spectral response range of InGaAs detector was 0.95 to 1.7 μm. The formation of the absorption peaks at 330 and 460 nm occurred at the same rate constant (k) of 1.1×10^8 s^{-1}, while two bands at 330 and 460 nm showed different decay kinetics (Figure 3, inset). Therefore, it is suggested that two bands at 330 and 460 nm were assigned to two different species formed from 1,1,2,2-$Ph_4E^{\bullet-}$. The absorption bands at 330 and 460 nm are similar to those of diphenylmethyl radical ($Ph_2CH^{\bullet}$)[6] and $Ph_2C^-(CH_2)_3CH_3$,[31] respectively. Although the absorption of diphenylmethyl anion (Ph_2CH^-) has not been reported, it is probably similar to that of $Ph_2C^-(CH_2)_3CH_3$. It has been reported that mesolysis of 1,1,2,2-tetraalkyl-1-(4′-nitrophenyl)-2-phenylethane radical anion produces the corresponding tertiary benzylic radical and anion.[10] Therefore, it is concluded that $Ph_2CH^{\bullet}$ and Ph_2CH^- with absorption bands at 330 and 460 nm, respectively, are produced from the mesolysis of 1,1,2,2-$Ph_4E^{\bullet-}$ with $k_{meso} = 1.1 \times 10^8$ s^{-1} (eq 4).

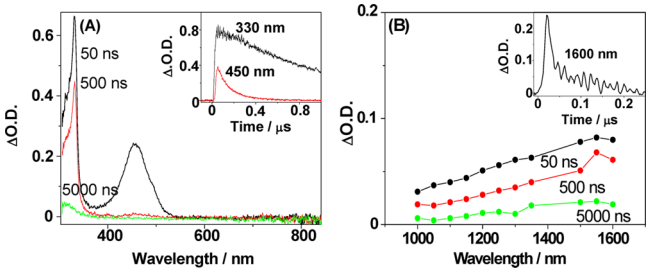

Figure 3. Transient absorption spectra observed at 50, 500, and 5000 ns after an electron pulse during the pulse radiolysis of 1,1,2,2-Ph_4E (1.0×10^{-2} M) in Ar-saturated MTHF (A) in the UV−visible region and (B) in the NIR region at 295 K. Insets show time profiles of the transient absorption at 330 (black) and 450 nm (red) (A), 1600 nm (B) after an electron pulse.

$$1,1,2,2\text{-}Ph_4E + e_s^- \rightarrow 1,1,2,2\text{-}Ph_4E^{\bullet-} \xrightarrow{k_{meso}} Ph_2CH^{\bullet} + Ph_2CH^- \quad (4)$$

In the case of Ph_3E, $Ph_3E^{\bullet-}$ showed two CR bands due to apparent 1,1-dimer radical anion and weak 1,2-dimer radical anion at 77 K.[30] Increasing temperature to 100 K, the CR bands disappeared with no band formation. No characteristic

dx.doi.org/10.1021/jo301853g | J. Org. Chem. 2013, 78, 1887−1893

absorption of $Ph_2CH^•$ or Ph_2CH^- was observed after an 8-ns electron pulse during the pulse radiolysis of Ph_3E in MTHF at room temperature, indicating no mesolysis of $Ph_3E^{•-}$ occurs.

Mesolysis of $Ph_5E^{•-}$, $Ph_6E^{•-}$, and 1,1,1,2-$Ph_4E^{•-}$ Having 1,1,1-Triphenylmethyl Chromophore. Figure 4 shows

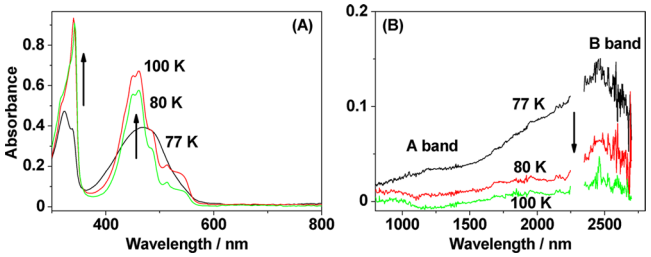

Figure 4. Absorption spectrum observed after the γ-radiolysis of Ph_5E (1.0×10^{-2} M) in MTHF rigid glass at 77 K and increasing temperature to 100 K (A) in the UV–visible region and (B) in the NIR region.

absorption spectra of $Ph_5E^{•-}$ observed after the γ-radiolysis of Ph_5E in MTHF rigid glass at 77 K. The bands around 320 and 480 nm were observed in the UV–visible region, while two intramolecular CR bands (A and B bands) appeared in the NIR region at 77 K.[30] Increasing temperature from 77 to 100 K, the band at 480 nm and CR bands of $Ph_5E^{•-}$ disappeared together with formation of two sharp absorption peaks at 340 and 460 nm (Figure 4).

The transient absorption spectra were observed at various times after an 8-ns electron pulse during the pulse radiolysis of Ph_5E in MTHF at room temperature as shown in Figure 5.

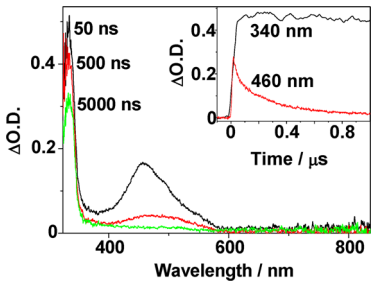

Figure 5. Transient absorption spectra observed at 50, 500, and 5000 ns after an electron pulse during the pulse radiolysis of Ph_5E (1.0×10^{-2} M) in MTHF at 295 K. Inset shows time profiles of the transient absorption at 340 (black) and 460 nm (red).

Neither band at 480 nm nor CR bands of $Ph_5E^{•-}$ was observed at 50 ns after pulse, while two absorption peaks at 340 and 460 nm were observed with different decay kinetics (Figure 5, inset).

The absorption band at 340 nm is similar to that of triphenylmethyl radical ($Ph_3C^•$) formed from the C–O bond dissociation of triphenylmethanol by the γ-irradiation,[32] while that at 460 nm is similar to that of Ph_2CH^- formed from the mesolysis of 1,1,2,2-$Ph_4E^{•-}$. Since the mesolysis is a thermal process, it does not occur in MTHF rigid glass at 77 K. Therefore, the absorption spectral changes in Figure 4a indicated that two bands at 340 and 460 nm were assigned to $Ph_3C^•$ and Ph_2CH^-, respectively, produced from the mesolysis of $Ph_5E^{•-}$. On the other hand, the formation of $Ph_3C^•$ and Ph_2CH^- was observed with disappearance of the absorption band at 480 nm. These results suggest that the absorption band at 480 nm is reasonably assigned to the local excitation (LE) band of $Ph_5E^{•-}$. The k_{meso} at room temperature was estimated to be $\gg 10^8$ s^{-1} which is larger than the experimental limit (eq 5). The mesolysis of $Ph_5E^{•-}$ occurs faster than that of 1,1,2,2-$Ph_4E^{•-}$.

$$Ph_5E + e_s^- \rightarrow Ph_5E^{•-} \rightarrow Ph_3C^• + Ph_2CH^- \quad (5)$$

Supporting Information Figure S1 shows absorption spectra of 1,1,1,2-$Ph_4E^{•-}$ observed after the γ-radiolysis of 1,1,1,2-Ph_4E in MTHF rigid glass at 77 K, where no band was observed in the UV–visible region. The absorption spectrum of 1,1,1,2-$Ph_4E^{•-}$ showed two strong A bands and a weak B band of intramolecular CR bands in the NIR region at 77 K. Increasing temperature to 100 K, neither $Ph_3C^•$ nor other absorption bands were observed. The absorption band at 510 nm was observed immediately after an electron pulse during the pulse radiolysis of 1,1,1,2-Ph_4E in MTHF at room temperature as shown in Supporting Information Figure S2. The absorption band at 510 nm disappeared at the decay rate constant of 2.6×10^6 s^{-1} without formation of $Ph_2CH^•$ or Ph_2CH^-, indicating no mesolysis of 1,1,1,2-$Ph_4E^{•-}$ occurs at room temperature. Since the absorption band at 510 nm was similar to that at 480 nm observed for $Ph_5E^{•-}$ at 77 K, it is assigned to the LE band of 1,1,1,2-$Ph_4E^{•-}$.

Figure 6A shows absorption spectra observed after the γ-radiolysis of Ph_6E in MTHF rigid glass at 77 K. The CR band

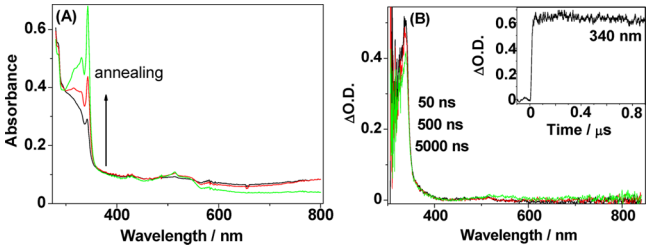

Figure 6. (A) Absorption spectrum observed after the γ-radiolysis of Ph_6E (1.0×10^{-2} M) in MTHF rigid matrix at 77 K. (B) Transient absorption spectra observed at 50, 500, and 5000 ns after a electron pulse during the pulse radiolysis of Ph_6E (1.0×10^{-2} M) in MTHF at 295 K. Inset is time profile of the transient absorption at 340 nm.

was not observed in the NIR region. The absorption bands at 340 and 500 nm in the UV–visible region were observed at 77 K. The absorption band at 340 nm was similar to that of $Ph_3C^•$. The weak absorption at 500 nm is similar to that of $Ph_3C^-Li^+$,[33] although the absorption of free Ph_3C^- has not been reported. Therefore, two bands at 340 and 500 nm were assigned to $Ph_3C^•$ and Ph_3C^-, respectively. Increasing temperature from 77 to 100 K, two bands of $Ph_3C^•$ and Ph_3C^- increased (Figure 6A). The band of $Ph_3C^•$ at 340 nm was observed immediately after an electron pulse during the pulse radiolysis of Ph_6E in MTHF at room temperature as shown in Figure 6B. However, the absorption of free Ph_3C^- was not observed, indicating that free Ph_3C^- is an unstable species in solution at room temperature. In fact, Ph_3C^- ion pair with alkali metal ($Ph_3C^-M^+$) is observed only at low temperature below 220 K.[33,34]

One electron attachment of Ph_6E was followed by the subsequent dissociation to $Ph_3C^•$ and Ph_3C^- without formation of $Ph_6E^{•-}$ involving intramolecular charge delocalization (eq 6). Since negative charge is efficiently delocalized in π-chromophores and central C–C σ bond in $Ph_6E^{•-}$, one electron

dx.doi.org/10.1021/jo301853g | J. Org. Chem. 2013, 78, 1887–1893

reduction of Ph_6E is followed by the subsequent C−C σ bond dissociation. In other words, the mesolysis of $Ph_6E^{\bullet-}$ occurs with a large k_{meso}.

$$Ph_6E + e_s^- \rightarrow Ph_3C^{\bullet} + Ph_3C^- \quad (6)$$

Intramolecular Charge Delocalization and Mesolysis. The absorption spectra of 1,1,2,2-$Ph_4E^{\bullet-}$ at 77 K showed two CR interactions between two phenyl groups at 1,1- and 1,2-positions, suggesting that negative charge (SOMO unpaired electron) of 1,1,2,2-$Ph_4E^{\bullet-}$ is delocalized on 1,1,2,2-Ph_4E having four phenyl groups as shown in Figure 7 (ωB97XD/6-31+G(d)).[30] The central C−C bond distance of 1,1,2,2-$Ph_4E^{\bullet-}$ (1.5827 Å) is longer than that of neutral 1,1,2,2-Ph_4E (1.5540 Å).

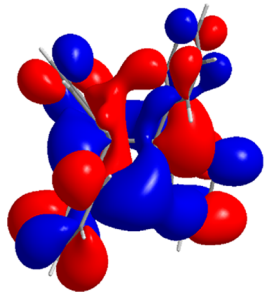

Figure 7. SOMO of 1,1,2,2-$Ph_4E^{\bullet-}$. Reprinted from ref 30. Copyright 2012 American Chemical Society.

On the basis of the results of the γ-radiolysis, the negative charge delocalization of 1,1,2,2-$Ph_4E^{\bullet-}$ can be illustrated by I, II, and III equilibrium states as shown in Scheme 1,[30] where I denotes 1,2-dimer radical anion and II and III denote 1,1-dimer radical anions. No formation of $Ph_2CH^{\bullet}$ and Ph_2CH^- was observed with the disappearance of I. Therefore, the mesolysis of 1,1,2,2-$Ph_4E^{\bullet-}$ is resulted from II or III where the negative charge is delocalized in the π^* orbital of two phenyl groups and C−C σ^* orbital. The C−C σ bond dissociation occurs to yield carbon radical and carboanion, that is, $Ph_2CH^{\bullet}$ and Ph_2CH^-, respectively.

The interaction between $\pi-\sigma$ in $Ph_5E^{\bullet-}$ with 2,2-diphenylmethyl chromophore is stronger than that in 1,1,2,2-$Ph_4E^{\bullet-}$ with 1,1-diphenylmethyl chromophore. The bond dissociation energy (BDE) of the C−C σ bond shows that the dissociation of $Ph_5E^{\bullet-}$ is exothermic in the gas phase (Table 2). The interaction between phenyl groups and C−C σ bond might be responsible for the small BDE for $Ph_5E^{\bullet-}$. In addition, the central C−C σ bond distance of $Ph_5E^{\bullet-}$ (1.60558 Å) is longer than that of $Ph_4E^{\bullet-}$. Slightly increasing temperature leads softening of the MTHF rigid glass, and the mesolysis of $Ph_5E^{\bullet-}$ occurs to give $Ph_3C^{\bullet}$ and Ph_2CH^-. The other dissociation of $Ph_5E^{\bullet-}$ to give $Ph_2CH^{\bullet}$ and Ph_3C^- does not occur, since no formation of $Ph_2CH^{\bullet}$ with absorption peak at 330 nm was observed. The negative charge delocalization of $Ph_5E^{\bullet-}$ can be illustrated by IV, V, and VI equilibrium states as shown in Scheme 2,[30] where IV, V, and VI denote 1,2-, 1,1-, and 2,2-dimer radical anions, respectively. No formation of $Ph_3C^{\bullet}$ and Ph_2CH^- was observed with the disappearance of IV and V. The mesolysis of $Ph_5E^{\bullet-}$ is resulted from VI where the negative charge is delocalized in the π^* orbital of two phenyl groups and C−C σ^* orbital. The C−C σ bond dissociation occurs to yield $Ph_3C^{\bullet}$ and Ph_2CH^-. It should be noted that II, III, VI are responsible for the mesolysis, but V is not. The result suggests that the electronic and steric effects are important in the negative charge delocalization in the π^* orbital of two phenyl groups and C−C σ^* orbital for the mesolyses of 1,1,2,2-$Ph_4E^{\bullet-}$ and $Ph_5E^{\bullet-}$.

In the case of 1,1,1,2-$Ph_4E^{\bullet-}$, negative charge is delocalized in four phenyl groups of 1,1,1,2-Ph_4E at 77 K. Since no absorption band of benzyl radical at 320 nm was observed even at room temperature, no dissociation occurs. The central C−C bond distance of 1,1,1,2-$Ph_4E^{\bullet-}$ (1.59212 Å) is longer that of 1,1,2,2-$Ph_4E^{\bullet-}$ (1.58270 Å) because of the steric hindrance of three phenyl groups at C1. However, the BDE of 1,1,1,2-$Ph_4E^{\bullet-}$ (16.7 kcal mol^{-1}) is larger than that of 1,1,2,2-$Ph_4E^{\bullet-}$ (10.8 kcal mol^{-1}) in gas phase. The negative charge is not sufficiently delocalized in the π^* orbital of two phenyl groups and C−C σ^* orbital of 1,1,2,2-$Ph_4E^{\bullet-}$ compared with II and III of 1,1,2,2-$Ph_4E^{\bullet-}$ and VI of $Ph_5E^{\bullet-}$. Thus, no mesolysis of 1,1,1,2-$Ph_4E^{\bullet-}$ occurs even at room temperature.

In the case of Ph_6E, the central C−C bond distance is significantly longer than that of other Ph_nE because of the large steric hindrance between six phenyl groups.[35] Although energy minimized structure was not obtained in spite of several attempts, it is expected that the central C−C BDE is much smaller and the central C−C bond distance is much longer in $Ph_6E^{\bullet-}$ than in Ph_6E. The one electron attachment of Ph_6E was followed by the subsequent dissociation to give $Ph_3C^{\bullet}$ and Ph_3C^- without formation of $Ph_6E^{\bullet-}$ involving intramolecular radical anion at 77 K.

Accordingly, k_{meso} increases in the order of $Ph_3E^{\bullet-}$, 1,1,1,2-$Ph_4E^{\bullet-}$ ≪ 1,1,2,2-$Ph_4E^{\bullet-}$ < $Ph_5E^{\bullet-}$ < $Ph_6E^{\bullet-}$ which is nearly consistent with the steric hindrance of phenyl groups in the order of $Ph_3E^{\bullet-}$ < $Ph_4E^{\bullet-}$ < $Ph_5E^{\bullet-}$ < $Ph_6E^{\bullet-}$. In addition, large interaction between phenyl π^* orbital and C−C σ^* orbital, or the negative charge delocalization in phenyl groups and C−C σ bond in $Ph_nE^{\bullet-}$ must be responsible for k_{meso}. When interaction between phenyl π^* orbital and C−C σ^* orbital is larger and negative charge is more delocalized in the central C−C bond of $Ph_nE^{\bullet-}$, k_{meso} is larger.

Temperature Dependence of Mesolysis. The temperature dependence of the formation rate constant (k_f) for Ph_2CH^- was examined in the range from 210 to 295 K for the mesolysis of 1,1,2,2-$Ph_4E^{\bullet-}$. The decay rate constant (k_d) of 1,1,2,2-$Ph_4E^{\bullet-}$ and k_f of $Ph_2CH^{\bullet}$ were not measured because time profiles of the transient absorption at 1500 and 330 nm

Scheme 1. Negative Charge Delocalization and Mesolysis of 1,1,2,2-$Ph_4E^{\bullet-}$

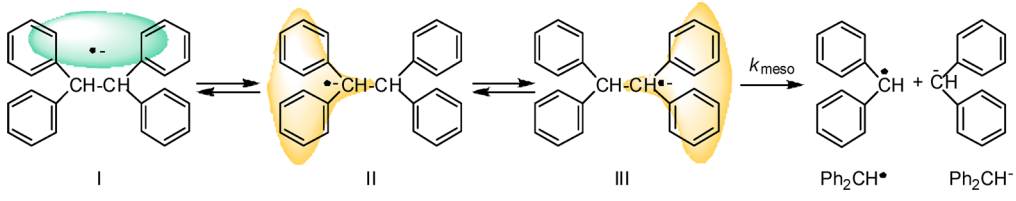

dx.doi.org/10.1021/jo301853g | J. Org. Chem. 2013, 78, 1887−1893

Scheme 2. Negative Charge Delocalization and Mesolysis of $Ph_5E^{\bullet-}$

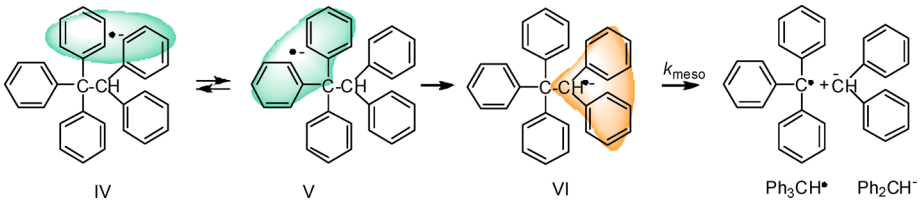

were very noisy at low temperature region (210−250 K). On the other hand, the k_{f460} values were obtained within ±5% error and listed in Table 1. The k_{f460} is expressed by eq 7,

$$\ln k_{f460} = \ln A_{460} - \Delta E_{a460}(RT)^{-1} \quad (7)$$

Table 1. Formation Rate Constants of Ph_2CH^- Obtained at Various Temperatures for Mesolysis of 1,1,2,2-$Ph_4E^{\bullet-}$

T^a/K	$k_{f460}{}^b/10^7$ s^{-1}
295	11
275	7.1
250	3.7
225	1.9
210	1.7

^{a}±1.0 °C. ^{b}Error ±5%.

where A_{460} and ΔE_{a460} denote a frequency factor and an apparent activation energy, respectively, for the mesolysis of 1,1,2,2-$Ph_4E^{\bullet-}$. Figure 8 shows the Arrhenius plots of k_{f460} with a

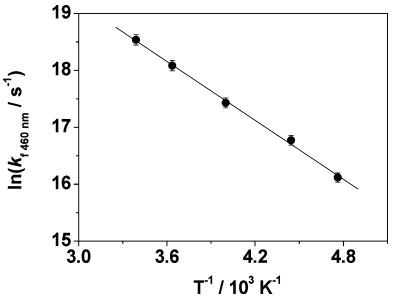

Figure 8. Arrhenius plots of the formation rate constants, k_f of Ph_2CH^- obtained during the pulse radiolysis of 1,1,2,2-Ph_4E (1.0×10^{-2} M) in MTHF in the temperature range 210−295 K.

fitted line. From the slope and intercept of the line, ΔE_{a460} and A_{460} for the mesolysis of 1,1,2,2-$Ph_4E^{\bullet-}$ were determined to be 3.3 kcal mol^{-1} and 3.9×10^{10} s^{-1}, respectively.

Similarly, the temperature dependence of k_f for $Ph_3C^{\bullet}$ and Ph_2CH^- was examined for the mesolysis of $Ph_5E^{\bullet-}$ in the range from 120 to 175 K. From the Arrhenius plots (Figure S3), ΔE_a and A were determined to be 3.8 kcal mol^{-1} and 6.5×10^{12} s^{-1}, respectively. The ΔE_a values of 1,1,2,2-$Ph_4E^{\bullet-}$ and $Ph_5E^{\bullet-}$ were similar to each other, while the A for $Ph_5E^{\bullet-}$ is two order larger than that of 1,1,2,2-$Ph_4E^{\bullet-}$.

Mesolysis of Polyphenylethane Radical Cations ($Ph_nE^{\bullet+}$). It is established that radiolysis of Ph_nE in halogenated alkanes causes one electron oxidation of Ph_nE via hole trapping to give $Ph_nE^{\bullet+}$ (eqs 8−10).[11]

$$R\text{-}Cl \rightsquigarrow RCl^{\bullet+} + e_s^- \quad (8)$$

$$e_s^- + RCl \rightarrow R^{\bullet} + Cl^- \quad (9)$$

$$RCl^{\bullet+} + Ph_nE \rightarrow Ph_nE^{\bullet+} + RCl \quad (10)$$

The transient absorption spectra were recorded at various times after an 8-ns electron pulse during the pulse radiolysis of 1,1,2,2-Ph_4E in 1,2-dichloroethane (DCE) at room temperature under Ar atmosphere (Figure 9). The transient absorptions of

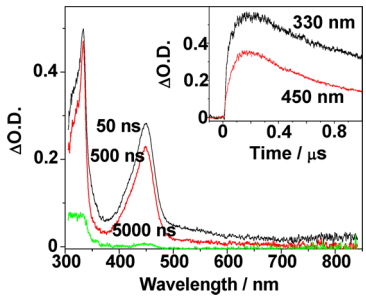

Figure 9. Transient absorption spectra observed at 50, 500, and 5000 ns after a electron pulse during the pulse radiolysis of 1,1,2,2-Ph_4E 1.0 $\times 10^{-2}$ M in DCE at 295 K. Inset shows time profiles of the transient absorption at 330 (black) and 450 nm (red).

$Ph_2CH^{\bullet}$ and diphenylmethyl cation (Ph_2CH^+) were observed with the formation of two absorption peaks at 330 and 460 nm at the same rate constant of $k_f = 1.4 \times 10^7$ s^{-1} at room temperature (eq 11).[6] Since the formation of $Ph_2CH^{\bullet}$ and Ph_2CH^+ is resulted from the mesolysis of 1,1,2,2-$Ph_4E^{\bullet+}$, $k_f = k_{meso}$. The k_{meso} for 1,1,2,2-$Ph_4E^{\bullet+}$ was ten folds smaller than that for 1,1,2,2-$Ph_4E^{\bullet-}$.

$$1,1,2,2\text{-}Ph_4E^{\bullet-} \xrightarrow{k_{meso}} Ph_2CH^{\bullet} + Ph_2CH^+ \quad (11)$$

In general, benzene radical cation forms a dimer radical cation in which positive charge is delocalized between two benzene molecules.[36] The stabilization of positive charge by the CR interaction in dimer radical cations is larger than that of negative charge in dimer radical anion. For example, the stabilization energy (E_{CR}) of [3.2](1,4)cyclophane radical cation (73.9 kJ/mol) is larger than that of the corresponding radical anion (56.9 kJ mol^{-1}).[37,38] Similarly, higher stabilization of positive charge in $Ph_nE^{\bullet+}$ than that of negative charge in $Ph_nE^{\bullet-}$ is responsible for the smaller k_{meso} for $Ph_nE^{\bullet+}$ than those for $Ph_nE^{\bullet-}$. In other words, higher activation energy is necessary to have enough large interaction between π orbital and C−C σ orbital, or enough positive charge delocalization in phenyl groups and C−C σ bond for the mesolysis of $Ph_nE^{\bullet+}$, compared with $Ph_nE^{\bullet-}$.

In the mesolysis of 1,1,1,2-$Ph_4E^{\bullet+}$, formation of Ph_3C^+ with absorption peak at 415 nm and benzyl radical was observed (Supporting Information Figure S4).[7,39] The k_{meso} for 1,1,1,2-$Ph_4E^{\bullet+}$ was ten folds larger than that for 1,1,2,2-$Ph_4E^{\bullet+}$. This is consistent with the BDE of 1,1,1,2-$Ph_4E^{\bullet+}$ smaller than that of 1,1,2,2-$Ph_4E^{\bullet+}$ due to steric hindrance of triphenylmethyl chromophore. Similarly, in the case of $Ph_5E^{\bullet+}$ and $Ph_6E^{\bullet+}$, the

dx.doi.org/10.1021/jo301853g | J. Org. Chem. 2013, 78, 1887−1893

Table 2. Central C−C Distance (r), Mesolysis Rate Constants (k_{meso}) and C−C BDE of $Ph_nE^{\bullet-}$ and $Ph_nE^{\bullet+}$

	neutral	radical anion			radical cation		
Ph_nE	r/Å	r/Å	k_{meso}[a]/ s^{-1}	BDE[b]	r/Å	k_{meso}[a]/ s^{-1}	BDE[b]
Ph_3E	1.54806	1.57951	~0	23.8	1.53481	~0	39.5
1,1,2,2-Ph_4E	1.55400	1.58270	1.1×10^8	10.8	1.54420	1.4×10^7	21.1
1,1,1,2-Ph_4E	1.56819	1.59212	~0	16.7	1.55836	$>2 \times 10^8$	8.75
Ph_5E	1.59868	1.60558	$>2 \times 10^8$	−2.9	1.58448	$>2 \times 10^8$	−0.85
Ph_6E	1.70000[c]	−[d]	concerted	−[d]	−[d]	1.9×10^6	−[d]

[a]At room temperature. [b]In kcal mol^{-1}. [c]Reference 35. [d]Not calculated.

formations of Ph_3C^+ at 415 nm and $Ph_2CH^{\bullet}$ or $Ph_3C^{\bullet}$ were observed, respectively, indicating the mesolysis (Supporting Information Figures S5 and S6). The mesolysis of $Ph_nE^{\bullet+}$ having 1,1,1-triphenylmethyl chromophore occurs to give Ph_3C^+ and corresponding phenyl methyl radical. The k_{meso} for $Ph_5E^{\bullet+}$ and $Ph_6E^{\bullet+}$ are equivalent or smaller than that of 1,1,1,2-$Ph_4E^{\bullet+}$, while the BDEs of $Ph_5E^{\bullet+}$ and $Ph_6E^{\bullet+}$ are smaller than that of 1,1,1,2-$Ph_4E^{\bullet+}$ (Table 2). The positive charge is stabilized by the CR interactions in the triphenylmethyl chromophore between three phenyl groups. It is reported that benzene radical cation forms a trimer radical cation in which positive charge is delocalized in three benzene moleucles.[40,41] The positive charge delocalization might be more efficient in triphenylmethyl chromophore than in diphenylmethyl chromophore. The mesolysis of $Ph_5E^{\bullet+}$ having 1,1,1-triphenylmethyl chromophore occurs predominantly through the thermodynamically favored pathway to generate Ph_3C^+ and $Ph_2CH^{\bullet}$.

CONCLUSIONS

The mesolysis of $Ph_nE^{\bullet-}$ such as 1,1,2,2-$Ph_4E^{\bullet-}$ and $Ph_5E^{\bullet-}$ occurs via stepwise mechanism involving of $Ph_nE^{\bullet-}$ in which negative charge is delocalized to give intramolecular dimer radical anions. The mesolysis, the nonpolar C−C bond dissociation of $Ph_nE^{\bullet-}$ is explained by the BDE of the central C−C σ bond and negative charge delocalization in phenyl groups and C−C σ bond. Such interaction or delocalization is preferable in 1,2-dimer radical anion of $Ph_nE^{\bullet-}$. In other words, the negative charge delocalization between two phenyl groups as the intramolecular dimer radical anion or in phenyl groups and C−C σ bond is the important factor for the mesolysis of $Ph_nE^{\bullet-}$. It should be noted that k_{meso} values for $Ph_nE^{\bullet+}$ are smaller than those for $Ph_nE^{\bullet-}$. The difference is explained by higher stabilization of positive charge in $Ph_nE^{\bullet+}$ than that of negative charge in $Ph_nE^{\bullet-}$. To understand the nonpolar C−C σ bond dissociation of radical anions of aromatic hydrocarbons in general, further studies for various aromatic hydrocarbons having bulky and long chain length are in progress.

EXPERIMENTAL SECTION

Materials. 1,1,2,2-Tetraphenylethane (1,1,2,2-Ph_4E) and 1,1,2-triphenylethane (Ph_3E) were synthesized by hydrogenation of the corresponding olefin by Pd/C in ethanol. These phenylalkanes were purified by column chromatography (Silica gel). 1,1,1,2-Tetraphenylethane (1,1,1,2-Ph_4E) was used without further purification. 1,1,1,2,2-Pentaphenylethane (Ph_5E) and 1,1,1,2,2,2-hexaphenylethane (Ph_6E) are known compounds, and were prepared by a method similar to that reported by Smith.[42] 2-Methyltetrahydrofuran (MTHF) was distilled over CaH_2 before use. Spectral grade 1,2-dichloroethane (DCE) was used as solvent without further purification.

Pulse Radiolysis. Pulse radiolysis experiments were performed using an electron pulse (27 MeV, 8 ns, 0.87 kGy per pulse) from a linear accelerator at Osaka University. MTHF solutions of polyphenylethane (Ph_nE) were degassed by the freeze−pump−thaw cycles on a high vacuum line (5×10^4 Torr) and sealed in a Suprasil cell ($10 \times 10 \times 40$ mm^3). The samples were transferred into an Oxford Optistat DN704 cryostat with flat sapphire windows with a digital temperature controller (DTC-2). The temperature was raised from 120 K, and was stabilized within ±0.5 K for at least 1 min before each measurement. The kinetic measurements were performed using a nanosecond photoreaction analyzer system (Unisoku, TSP-1000). The monitor light was obtained from a pulsed 450-W Xe arc lamp (Ushio, UXL-451-0), which was operated by a large current pulsed-power supply that was synchronized with an electron pulse. The monitor light was passed through an iris with a diameter of 0.2 cm and sent into the sample solution at a perpendicular intersection to an electron pulse. The monitor light passing through the sample was focused on the entrance slit of a monochromator (Unisoku, MD200) and detected with a photomultiplier tube (Hamamatsu Photonics, R2949). The transient absorption spectra were measured using a photodiode array (Hamamatsu Photonics, S3904−1024F) with a gated image intensifier (Hamamatsu Photonics, C2925-01) as a detector. The kinetic traces in NIR region were estimated using a fast InGaAs PIN photodiode (THORLABS PDA255) with a monochromator (Jobin Yvon, TRIAX190) and the transient digitizer (Tektronix, TDS580D). The total system was controlled with a personal computer via GPIB interface.

γ-Radiolysis. The γ-radiolysis of MTHF rigid glass degassed by the freeze−pump−thaw method was carried out in 1 mm thick Suprasil cells in liquid nitrogen at 77 K by a ^{60}Co γ source (total dose, 1.54 kGy). The absorption spectra were measured in Dewar vessel at 77 K by a with UV−vis-NIR spectrometer (Shimadzu UV-3100) and with VIS spectrometer (Shimadzu multispec-1500). The absorption spectrum was noisy in the longer wavelength region than 2200 nm because of the overlap with the vibrational overtone of MTHF.

Theoretical Calculations. The central C−C bond distances and BDE values of phenylalkanes radical ion and neutral alkanes of were estimated by DFT-D at the ωB97XD/6-31+G(d) level using Gaussian09 package.[43]

ASSOCIATED CONTENT

Supporting Information

Absorption spectrum observed after the γ-radiolysis of 1,1,1,2-$Ph_4E^{\bullet-}$ in MTHF in NIR region. Arrhenius plots of the formation rate constants, k_f of Ph_2CH^- and $Ph_3C^{\bullet}$ obtained during the pulse radiolysis of Ph_5E in MTHF. Transient absorption spectra observed after an during the pulse radiolysis of Ph_5E, Ph_5E, and 1,1,1,2-Ph_4E in DCE. Optimized structures of Ph_nE, $Ph_nE^{\bullet-}$ and $Ph_nE^{\bullet+}$. This material is available free of charge via the Internet at http://pubs.acs.org.

AUTHOR INFORMATION

Corresponding Author

*Fax: +81-6-6879-8499. Tel: +81-6-6879-8495. E-mail: majima@sanken.osaka-u.ac.jp

Notes

The authors declare no competing financial interest.

■ ACKNOWLEDGMENTS

We thank the members of the Research Laboratory for Quantum Beam Science of ISIR, Osaka University for assistance in the γ-ray radiolysis and pulse radiolysis experiments. We are grateful to Prof. Akira Sugimoto and Dr. Takumi Kimura (ISIR, Osaka University) for synthesis of compounds. This work has been partly supported by a Grant-in-Aid for Scientific Research (Project 22245022 and others) from the Ministry of Education, Culture, Sports, Science and Technology (MEXT) of Japanese Government. S.T. thanks the Special Coordination Funds for Promoting Science and Technology from MEXT for the Osaka University Program for the Support of Networking among Present and Future Women Researchers. T.M. thanks the World Class University program funded by the Ministry of Education, Science and Technology through the National Research Foundation of Korea (R31-2011-000-10035-0) for support.

■ REFERENCES

(1) Maslak, P.; Narvaez, J. N. *Angew. Chem.* **1990**, *102*, 302.
(2) Baciocchi, E.; Bietti, M.; Lanzalunga, O. *Acc. Chem. Res.* **2000**, *33*, 243.
(3) Saveant, J. M. *Acc. Chem. Res.* **1993**, *26*, 455.
(4) Houmam, A. *Chem. Rev.* **2008**, *108*, 2180.
(5) Braieda, B.; Thogersen, L.; Wu, W.; Hiberty, P. C. *J. Am. Chem. Soc.* **2002**, *124*, 11781.
(6) Faria, J. L.; McClelland, R. A.; Steenken, S. *Chem.—Eur. J.* **1998**, *4*, 1275.
(7) Del Giacco, T.; Lanzalunga, O.; Mazzonna, M.; Mencarelli, P. *J. Org. Chem.* **2012**, *77*, 1843.
(8) Baciocchi, E.; Bettoni, M.; Del Giacco, T.; Lanzalunga, O.; Mazzonna, M.; Mencarelli, P. *J. Org. Chem.* **2011**, *76*, 573.
(9) Baciocchi, E.; Del Giacco, T.; Elisei, F.; Lapi, A. *J. Org. Chem.* **2006**, *71*, 853.
(10) Maslak, P.; Narvaez, J. N.; Vallombroso, T. M., Jr. *J. Am. Chem. Soc.* **1995**, *117*, 12373.
(11) Balzani, V., Ed. *Electron Transfer in Chemistry*, Volume *1*; Wiley-VCH Verlag GmbH: New York, 2001; pp 502−554.
(12) Saeki, A.; Kozawa, T.; Ohnishi, Y.; Tagawa, S. *J. Phys. Chem. A* **2007**, *111*, 1229.
(13) Fujitsuka, M.; Samori, S.; Tojo, S.; Haley, M. M.; Majima, T. *ChemPlusChem* **2012**, *77*, 682.
(14) Higashino, S.; Saeki, A.; Okamoto, K.; Tagawa, S.; Kozawa, T. *J. Phys. Chem. A* **2010**, *114*, 8069.
(15) Antonello, S.; Maran, F. *Chem. Soc. Rev.* **2005**, *34*, 418.
(16) Costentin, C.; Robert, M.; Saveant, J.-M. *Chem. Phys.* **2006**, *324*, 40.
(17) Maran, F.; Wayner, D. D. M.; Workentin, M. S. *Adv. Phys. Org. Chem.* **2001**, *36*, 85.
(18) Kimura, N. *J. Am. Chem. Soc.* **2001**, *123*, 3824.
(19) Costentin, C.; Hapiot, P.; Medebielle, M.; Saveant, J.-M. *J. Am. Chem. Soc.* **2000**, *122*, 5623.
(20) Costentin, C.; Robert, M.; Saveant, J.-M. *J. Am. Chem. Soc.* **2004**, *126*, 16051.
(21) Maslak, P.; Guthrie, R. D. *J. Am. Chem. Soc.* **1986**, *108*, 2628.
(22) Pisano, L.; Farriol, M.; Asensio, X.; Gallardo, I.; Gonzalez-Lafont, A.; Lluch, J. M.; Marquet, J. *J. Am. Chem. Soc.* **2002**, *124*, 4708.
(23) Casado, F.; Pisano, L.; Farriol, M.; Gallardo, I.; Marquet, J.; Melloni, G. *J. Org. Chem.* **2000**, *65*, 322.
(24) Maslak, P.; Theroff, J. *J. Am. Chem. Soc.* **1996**, *118*, 7235.
(25) Maslak, P.; Narvaez, J. N. *J. Chem. Soc., Chem. Commun.* **1989**, 138.
(26) Antonello, S.; Daasbjerg, K.; Jensen, H.; Taddei, F.; Maran, F. *J. Am. Chem. Soc.* **2003**, *125*, 14905.
(27) Favaudon, V.; Tourbez, H.; Houee-Levin, C.; Lhoste, J. M. *Biochemistry* **1990**, *29*, 10978.
(28) Yamaji, M.; Tojo, S.; Takehira, K.; Tobita, S.; Fujitsuka, M.; Majima, T. *J. Phys. Chem. A* **2006**, *110*, 13487.
(29) Maslak, P.; Kula, J.; Narvaez, J. N. *J. Org. Chem.* **1990**, *55*, 2277.
(30) Tojo, S.; Fujitsuka, M.; Majima, T. *J. Org. Chem.* **2012**, *77*, 4932.
(31) Chang, C. J.; Kiesel, R. F.; Hogen-Esch, T. E. *J. Am. Chem. Soc.* **1975**, *97*, 2805.
(32) Bromberg, A.; Meisel, D. *J. Phys. Chem.* **1985**, *89*, 2507.
(33) Buncel, E.; Menon, B. *J. Org. Chem.* **1979**, *44*, 317.
(34) Okano, M.; Kugita, T.; Ohtani, D.; Hamano, H. *Bull. Chem. Soc. Jpn.* **1995**, *68*, 759.
(35) Dames, E.; Sirjean, B.; Wang, H. *J. Phys. Chem. A* **2010**, *114*, 1161.
(36) Okamoto, K.; Seki, S.; Tagawa, S. *J. Phys. Chem. A* **2006**, *110*, 8073.
(37) Fujitsuka, M.; Tojo, S.; Shinmyozu, T.; Majima, T. *Chem. Commun. (Cambridge, U.K.)* **2009**, 1553.
(38) Fujitsuka, M.; Cho, D. W.; Tojo, S.; Yamashiro, S.; Shinmyozu, T.; Majima, T. *J. Phys. Chem. A* **2006**, *110*, 5735.
(39) Baidak, A.; Naumov, S.; Brede, O. *J. Phys. Chem. A* **2008**, *112*, 10200.
(40) Todo, M.; Okamoto, K.; Seki, S.; Tagawa, S. *Chem. Phys. Lett.* **2004**, *399*, 378.
(41) Fujitsuka, M.; Tojo, S.; Shibahara, M.; Watanabe, M.; Shinmyozu, T.; Majima, T. *J. Phys. Chem. A* **2011**, *115*, 741.
(42) Smith, W. B.; Harris, M. C. *J. Org. Chem.* **1983**, *48*, 4957.
(43) Frisch, M. J. T., G., W.; Schlegel, H. B.; Scuseria, G. E.; Robb, M. A.; Cheeseman, J. R.; Scalmani, G.; Barone, V.; Mennucci, B.; Petersson, G. A.; Nakatsuji, H.; Caricato, M.; Li, X.; Hratchian, H. P.; Izmaylov, A. F.; Bloino, J.; Zheng, G.; Sonnenberg, J. L.; Hada, M.; Ehara, M.; Toyota, K.; Fukuda, R.; Hasegawa, J.; Ishida, M.; Nakajima, T.; Honda, Y.; Kitao, O.; Nakai, H.; Vreven, T.; Montgomery, J. A. Jr.; Peralta, J. E.; Ogliaro, F.; Bearpark, M.; Heyd, J. J.; Brothers, E.; Kudin, K. N.; Staroverov, V. N.; Kobayashi, R.; Normand, J.; Raghavachari, K.; Rendell, A.; Burant, J. C.; Iyengar, S. S.; Tomasi, J.; Cossi, M.; Rega, N.; Millam, J. M.; Klene, M.; Knox, J. E.; Cross, J. B.; Bakken, V.; Adamo, C.; Jaramillo, J.; Gomperts, R.; Stratmann, R. E.; Yazyev, O.; Austin, A. J.; Cammi, R.; Pomelli, C.; Ochterski, J. W.; Martin, R. L.; Morokuma, K.; Zakrzewski, V. G.; Voth, G. A.; Salvador, P.; Dannenberg, J. J.; Dapprich, S.; Daniels, A. D.; Farkas, O.; Foresman, J. B.; Ortiz, J. V.; Cioslowski, J.; Fox, D. J. *Gaussian 09*; Gaussian, Inc.: Wallingford, CT, 2009.